

# On the FEM Treatment of Wedge Singularities in Waveguide Problems

Jaakko S. Juntunen and Theodoros D. Tsiboukis, *Member, IEEE*

**Abstract**—This paper introduces a novel extension to a scalar two-dimensional polynomial finite-element basis to better cope with wedge singularities in waveguide problems. An error estimate for the computed cutoff frequencies of the waveguide shows that the relative  $H^1$  error of the modal solution is critical. We demonstrate that the present extension significantly improves the approximation properties of a polynomial basis, especially in the  $H^1$  norm. Numerical examples show that the present extension compares well with other recent techniques. Combining variable order elements with singular basis extension provides further significant reduction of the computational burden.

**Index Terms**—High-order FEM methods, wedge singularities.

## I. INTRODUCTION

IN MODERN microwave and millimeter-wave technology, there exist many different devices based on microstrip lines. These include a variety of waveguides, patch antennas, filters, power dividers, directional couplers, etc. [1]. For design purposes, many diagrams and design aid formulas have been created (e.g., [2]). The microstrip line represents a realistic zero-angle wedge problem. More general wedges exist, for example, in corrugated structures. It is well known that, close to a wedge tip, the fields change rapidly and the transverse field components may even take infinite values [3]. However, in a homogeneous uniform cylindrical structure, the longitudinal components of the field are finite and belong to the space  $H^1$ , behaving as  $r^{1/2}$  in the most singular case. For such structures, the longitudinal components may be used as working variables. The field singularity problem at wedges is generally discussed in [3]–[5].

In [6], a low-order method is presented for solving the complete  $\vec{E}$ -field via scalar and vector potentials in two-dimensional (2-D) problems involving corners or highly curved surfaces. The methodology in [6] does not specifically take into account the field singularities, but assures spurious-free solutions of inhomogeneous wedge problems using a nodal finite-element basis. RMS errors of the order of few percents are reported. The infinite transverse field components are likely dominating sources of error, in the cases where the singularity is strong. Boyse *et al.* [6] solve some of the drawbacks reported earlier in [7].

The edge singularities of a zero-angle wedge are specially considered in a number of numerical techniques [8]–[10]. In [10], a few terms of an analytical expansion of the charge density on a microstrip line is used in a Green's function treatment for the evaluation of the capacitance of the line. The underlying assumptions are uniformity in one direction and quasi-TEM propagation. The development in [10] aims to evaluation of the characteristic impedance of the line, but the computed charge density could be used for the evaluation of the electric field as well. In [11], microstrip step discontinuities are considered via a certain mode-matching technique. Singular basis functions are also employed there.

A quasi-TEM analysis of arbitrary multiple conductor microwave transmission lines using the finite-element method (FEM) is discussed in [12]. A type of singular element is used there close to wedges, the elements being due to [13]. The singular elements used in [12] are almost the same than in [14] and [15]: the elements touching the wedge tip are modified locally to asymptotically incorporate the correct form of the singularity in the radial coordinate. To each node on or neighboring a singular wedge tip there is associated a singular basis function that replaces the corresponding linear basis function. The angular variation is not asymptotically accurate, however, in either [12], [14], or [15].

Supplementary singular basis functions are also proposed in [16], where they are associated only for the transverse-field components. It is true that the singularity of the longitudinal component is less severe, but based on the observations of this paper, it seems reasonable to consistently include the longitudinal singularity in the basis as well. An important property of the singular trial functions in [16] is that the curl of them is not more singular than the trial functions themselves [16, eq. (11)]. If it were, as could be incorrectly anticipated, the integration of the functional behind the variational procedure could not be performed and the inclusion of singular trial functions would fail. The trial functions in [16] are asymptotically accurate in both radial and angular coordinate. There are a few drawbacks: the singular basis functions are supported by the whole cross section of the waveguide, and the construction of them is not straightforward for such bases where degrees of freedom are not nodal values, e.g., hierarchic basis [17] used in this paper.

In [18] and [19], scalar singular elements and their properties are also discussed. The singular elements in [18] are constructed from six-node quadratic elements through a geometrical mapping of the reference triangle to the element space: the form of the basis functions in the reference triangle is standard and the singularity is introduced by the contraction property of the mapping close to the origin. The advantage of the method

Manuscript received March 25, 1999. This work was supported by the Finnish Graduate School of Electronics, Telecommunications and Automation, by the Tekniikan Edistämissäätiö Foundation, Finland, under a grant, and under EU Grant ERBFMBICT983 462.

J. S. Juntunen is with the Radio Laboratory, Helsinki University of Technology, FIN-02 015 HUT, Finland (e-mail: jaakko.juntunen@hut.fi).

T. D. Tsiboukis is with the Electrical and Computer Engineering Department, Aristotle University of Thessaloniki, GR-54 006 Thessaloniki, Greece.

Publisher Item Identifier S 0018-9480(00)04668-8.

is that the system size and form is unaffected, and the integration of the singular degrees of freedom is simply done by modifying the Jacobian of the singular mappings in the integration routine. Furthermore, the scheme is easily extendable to higher order bases, even to hierarchic ones. A few disadvantages exist, however. First, all the basis functions in the singular element are transformed and, in general, none of these remains polynomial. If the mode under investigation is smooth, we may lose the usual polynomial approximation and the convergence may be poor. Even if the mode has a singularity, a loss in the accuracy may happen because, in the most singular case where the longitudinal component takes the form  $\sqrt{r}$ , the second-order polynomials are effectively transformed to first-order ones. Another disadvantage is that the angular dependence is not accurately implemented. Gil and Zapata [18, Fig. 4] demonstrate that, for second-order basis, this is not a severe problem if the density of the elements is high enough in angular direction.

In [19], Gil and Zapata introduce a transition element that extends the range of the singularity in the computational model. The main anxiety was that the singular behavior extends a finite length from the singular point, and very small-sized singular elements cannot be used. In effect, the transition element makes the singular element larger in size and more complex by introducing new degrees of freedom. This corresponds closely to a single large-sized singular element with high-order polynomial part.

In [20] and [21], the field singularities near the tip of a conducting three-dimensional (3-D) cone are discussed. In a cone problem, the singularities are, in general, more severe than in a wedge problem. Like the transverse fields in a wedge problem, the fields in a cone problem drop from the  $\mathbf{H}^1$ , thus, the usual variational formulation of the Helmholtz equation is not possible, not even in a homogeneous problem. One can formulate the problem as a double-curl equation, ensuring that the curls of the trial fields belong to  $\mathbf{L}_2$ .

The origin of the well-known spurious solutions of the Maxwell's equations is discussed in [22]. The vector finite elements (or edge elements, see e.g., [23]–[29]) have been proposed primarily for the suppression of spurious modes. It is recalled in [29] that vector basis functions do not really suppress spurious modes, but identify them by associating the zero eigenvalue with them. Since the singularities are not implemented by any means in the usual vector elements, significant errors may be involved in a numerical solution that qualitatively seems to be physical and correct. Recently, in [30] and [31], the singularity is also implemented in vector elements. In [30], new basis functions are added to account for the singularity. The deficiency of [30] compared to this paper is that the basis in [30] is a low-order one, and it is not obvious how a high-order basis should be constructed. Also, angular variation is not accurately implemented. Many of the results reported in [30] can be computed using a scalar basis, namely, the wavenumbers of the homogeneous waveguides. Reference [31] involves a similar case. We propose that the higher terms in the series expansion of the asymptotic field [31, eq. (1a)] should be written more conveniently as

$$H_z = d_0 + d_1 r^\nu \cos(\nu\phi) + d_2 r^{2\nu} \cos(2\nu\phi) + \dots \quad (1)$$

Each term in (1) satisfies the Laplace equation in the cross section with a perfect electric conductor (PEC) boundary condition on the wedge, thus, any finite collection of terms represents a quasi-static mode.

Our experience suggests that the best performance is obtained by combination of singular elements and a variable-order basis. The latter is most easily realized through hierarchic polynomial basis [17]. There are also some additional advantages related to convergence analysis along the increased order of the basis, numerical stability, and condensation possibility of the so-called inner degrees of freedom, which reduces the system size considerably in quasi-TEM analysis of transmission lines and similar static problems. Thus, there still seems to remain a wide class of problems, e.g., homogeneous waveguides and (quasi-)TEM propagation mode analysis of transmission lines, where the scalar FEM is simpler and more efficient to use, as compared to vector finite elements. However, for a general 3-D singularity problem, the 3-D vector elements are probably the only choice. The singular vector elements in [30] and [31] could possibly be extended to the general case once the form and order of the singularity has been separately solved [20], [21].

In [32] and [33], modifications of the finite-difference time-domain (FDTD) method are presented for the wedge problem. In [33], the field is assumed to be expanded into an asymptotic series and the field values close to the wedge are fitted to the first few terms of the expansion to determine the expansion coefficients.

In this paper, a simple and computationally advantageous extension to a scalar 2-D polynomial finite-element basis is introduced to better cope with wedge singularities in waveguide problems. Although the discussion is limited to homogeneous problems, the basis extension can be adopted to any scalar basis and more general cases. Variable-order elements are used to further optimize the computation. The extension is constructed such that a small number of locally supported additional basis functions are joined into the polynomial basis. The extension has the correct asymptotic form in both radial and angular coordinates. Error estimation shows that the error of the eigenmodes in the  $\mathbf{H}^1$  norm is critical when evaluating the cutoff frequencies of a waveguide. It is demonstrated that the polynomials can poorly approximate the finite longitudinal fields close to the singularity in the  $\mathbf{H}^1$  norm, even though the approximation in the  $\mathbf{L}_2$  norm may seem satisfactory. Instead, the extended basis has very good approximation properties in both  $\mathbf{L}_2$  and  $\mathbf{H}^1$  norms. Several numerical examples are discussed that show considerable enhancement in the accuracy when compared to polynomial approximation. Comparisons are also provided with other singular basis function techniques.

## II. CONSTRUCTION OF THE BASIS EXTENSION

The dominating longitudinal wave component close to a wedge tip (Fig. 1) has a cross-sectional form in the  $r\phi$ -plane for the TM mode [33]

$$r^\nu \sin(\nu\phi) \quad (2)$$

and for the TE mode

$$r^\nu \cos(\nu\phi) \quad (3)$$

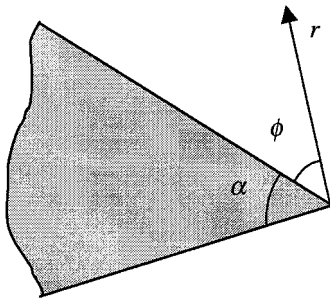


Fig. 1. Typical wedge geometry.

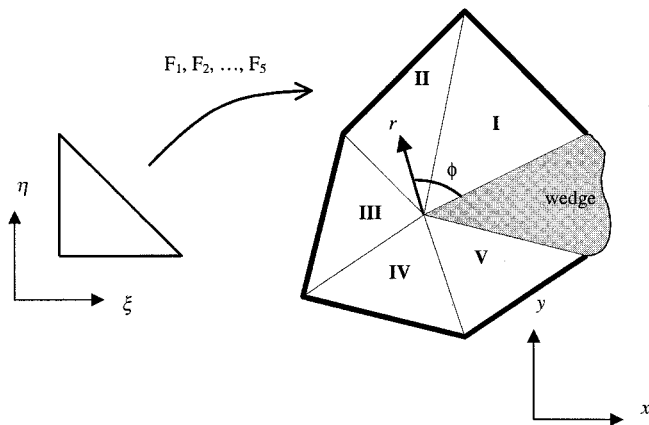


Fig. 2. Elements surrounding a singular wedge. Different coordinate systems.

where  $\nu = \pi/(2\pi - \alpha)$ . Here,  $\alpha$  is the wedge angle. In the most singular case,  $\alpha = 0$  and  $\nu = 1/2$ . Consider Fig. 2. Each of the five elements supports part of the extension function, each part being of the form

$$r^\nu \sin(\nu\phi) \cos\left(\frac{\pi}{2}(\xi + \eta)^2\right), \quad \text{for the TM mode} \quad (4)$$

and

$$r^\nu \cos(\nu\phi) \cos\left(\frac{\pi}{2}(\xi + \eta)^2\right), \quad \text{for the TE mode.} \quad (5)$$

Note that  $r, \phi$  are real coordinates in the physical space while  $\xi$  and  $\eta$  are coordinates in the reference triangle. Mapping  $F_i$  maps the reference triangle to the element  $i$ . In each of the mappings  $F_1, \dots, F_5$ , it is assumed that the origin  $\xi = 0, \eta = 0$  is mapped to the singular point—this is only a matter of local numbering of the nodes in the elements. Note that there is only one singular function associated to each singular point. Fig. 3 shows a contour plot of the TM extension function in the above case.

Close to the origin (= the singular point) the common cosine term in (4) and (5) equals unity up to the fourth order accuracy. Expanding in the polar coordinates of the reference triangle ( $\xi = R \cos \Theta, \eta = R \sin \Theta$ ), we have  $1 - \cos((\pi/2)(\xi + \eta)^2) = R^4(\pi^2/8)(\sin \Theta + \cos \Theta)^4 + 0(R^8)$ . This means that the singular basis function approximates the dominating term (2) or (3) very accurately in the immediate neighborhood of the singular point. On the other hand, along the thick line in Fig. 2, the cosine

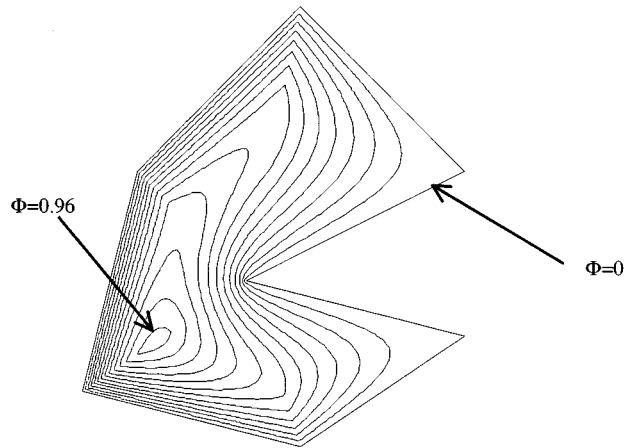


Fig. 3. Contour plot of the normalized singular basis function in the geometry of Fig. 2. Difference between contour lines is 0.08.

term is zero and, hence, the singular basis function is compactly supported.

Let us call the above-described singular basis function  $\Phi_1$ . We can include several other terms in the asymptotic series expansion of the field. The corresponding basis functions are constructed otherwise as  $\Phi_1$ , but their form in each of the supporting elements is

$$r^{n\nu} \left\{ \begin{array}{l} \sin(n\nu\phi) \\ \cos(n\nu\phi) \end{array} \right\} \cos\left(\frac{\pi}{2}(\xi + \eta)^2\right)$$

for  $\Phi_n$ . We will explicitly deal with  $\Phi_1, \Phi_2$ , and  $\Phi_3$ .

Higher power in the common cosine term would imply even closer approximation of the dominating term close to the singularity. Then, however, the cosine term would drop steeply to zero toward the edge  $\xi + \eta = 1$ . This is not desirable, and experiments with different powers suggest that the power two is close to optimal in most cases—the tradeoff between maximum accuracy close to the origin and minimum gradients close to the edge  $\xi + \eta = 1$  are then well balanced.

The polynomial part of our basis is a high-order hierarchical basis. As an example, we write down the complete set of third-order polynomial basis functions, defined over the standard triangle

$$\begin{aligned} f_1 &= 1 - \xi - \eta \\ f_2 &= \xi \\ f_3 &= \eta \\ f_4 &= \xi(1 - \xi - \eta) \\ f_5 &= \xi\eta \\ f_6 &= \eta(1 - \xi - \eta) \\ f_7 &= \xi(1 - \xi - \eta)(-1 + 2\xi) \\ f_8 &= \xi\eta(-1 + 2\eta) \\ f_9 &= \eta(1 - \xi - \eta)(1 - 2\eta) \\ f_{10} &= \xi\eta(1 - \xi - \eta). \end{aligned}$$

The functions  $\{f_1, f_2, f_3\}$  are called vertex modes,  $\{f_4, f_5, f_6\}$  are second-order side modes and  $\{f_7, f_8, f_9\}$  are third-order

side modes.  $f_{10}$  is called the third-order inner mode. Note that, except the vertex modes, the degrees of freedom are not directly related to nodal values. The term ‘‘hierarchical’’ means that if we want to ‘‘upgrade’’ the current basis to a fourth-order one, we simply add three fourth-order side modes and two fourth-order inner modes. In contrast, ‘‘upgrading’’ a third-order nodal basis to a fourth-order one requires redefinition of all the basis functions. For convergence analysis, a single high-order hierarchic system matrix contains all the lower order matrices as sub-matrices, and a single integration suffices.

Some results are presented for variable  $p$ -meshes also, where individual elements may be of different order. It is a significant advantage of the hierarchic system, that two neighboring elements supporting different order polynomials can easily be joined: a few side modes are simply deleted from the higher order element, associated to the edge joining the two elements. As a result, the higher order element next to the joint does not support a complete set of polynomials, while the low-order counterpart does. Of course, one can alternatively supply the low-order element with a few high-order side modes. In the computational point-of-view, the variable  $p$ -method proves to yield superior performance in terms of total computational burden compared to the uniform  $p$ -method.

We adopt the following terminology:  $\{\Phi_n\}$  is the set of all singular basis functions in the problem that are of type  $r^{n\nu} \begin{Bmatrix} \sin(n\nu\phi) \\ \cos(n\nu\phi) \end{Bmatrix}$ . Furthermore, we define the extended bases

Ext-1 = polynomial basis  $\cup \{\Phi_1\}$ .

Ext-12 = polynomial basis  $\cup \{\Phi_1\} \cup \{\Phi_2\}$ .

Ext-13 = polynomial basis  $\cup \{\Phi_1\} \cup \{\Phi_3\}$ .

Hence, if there are three singular points in the problem, the bases Ext-12 and Ext-13 contain six degrees of freedom more than the corresponding polynomial basis. In some problems, symmetry excludes  $\{\Phi_2\}$ , therefore, we also introduced Ext-13.

It must be emphasized that theoretically the inclusion of the singular basis functions cannot make the FEM solution worse in any circumstances. If a certain mode does not support a singularity, the corresponding coefficients simply vanish, and the remaining basis works as if no extension were made. However, if  $n\nu = \text{integer}$ ,  $\{\Phi_n\}$  is ‘‘almost’’ polynomial and may become essentially linearly dependent on the polynomial part, causing the matrices to be nearly singular. Indeed, loss of accuracy has been detected with very high-order bases, with  $\nu = 1/2$  and  $n = 2$ .

As a preliminary test, we chose  $\nu = 1/2$ , mapped the reference triangle onto itself, and projected (2) in  $L_2$  and  $H^1$  senses to the polynomial and the Ext-1 bases. Table I presents the results. Especially for high-order basis and  $H^1$  projection, the extension improves the approximation a lot. Note that numerical integration in polar coordinates is suggested in the projection.

### III. ERROR ESTIMATE FOR THE EIGENVALUES IN THE HELMHOLTZ EQUATION

Consider the scalar Helmholtz equation in a domain  $\Omega$

$$\nabla^2 \Phi + k^2 \Phi = 0. \quad (6)$$

TABLE I  
PROJECTION INTO STANDARD POLYNOMIAL AND EXT-1 BASES

| Order | $L_2$ -err. (poly)   | $L_2$ -err. (Ext-1)  | $H^1$ -err. (poly) | $H^1$ -err. (Ext-1)  |
|-------|----------------------|----------------------|--------------------|----------------------|
| $p=3$ | $1.41 \cdot 10^{-2}$ | $2.33 \cdot 10^{-3}$ | 0.1863             | 0.0285               |
| $p=5$ | $4.58 \cdot 10^{-3}$ | $5.67 \cdot 10^{-4}$ | 0.1192             | $7.54 \cdot 10^{-3}$ |
| $p=8$ | $1.45 \cdot 10^{-3}$ | $8.22 \cdot 10^{-6}$ | 0.0771             | $1.12 \cdot 10^{-3}$ |

Let us follow a standard variational principle to reformulate (6). For that, choose a proper finite dimensional test function space

$$V_h^0 = \text{span}\{\varphi_i\}_{i=1}^N \subset H^1(\Omega) \quad (7)$$

where the homogeneous Dirichlet or Neumann boundary conditions are implied in the basis functions. The infinite dimensional test function space is the whole  $H^1$  with imposed boundary conditions.

Let  $\Phi_h \in V_h^0$  denote the approximate solution to the problem, and let  $k_h^2$  be the corresponding eigenvalue. The approximate Galerkin solution is constructed such that for any  $\nu \in V_h^0$

$$\int_{\Omega} \nu \nabla^2 \Phi_h \, d\Omega + k_h^2 \int_{\Omega} \nu \Phi_h \, d\Omega = 0. \quad (8)$$

For the first integral, use Green’s formula to obtain

$$\begin{aligned} \int_{\Omega} \nu \nabla^2 \Phi_h \, d\Omega &= \int_{\Gamma} \nu \frac{\partial \Phi_h}{\partial n} \, d\Gamma - \int_{\Omega} \nabla \nu \cdot \nabla \Phi_h \, d\Omega \\ &= - \int_{\Omega} \nabla \nu \cdot \nabla \Phi_h \, d\Omega \end{aligned} \quad (9)$$

the last equality following from the Dirichlet boundary condition on  $\nu$  or Neumann boundary condition on  $\Phi_h$ , whichever is applicable. Hence, the eigenvalue can be written as

$$k_h^2 = \frac{\int_{\Omega} \nabla \nu \cdot \nabla \Phi_h \, d\Omega}{\int_{\Omega} \nu \Phi_h \, d\Omega} \quad (10)$$

for any nonzero  $\nu \in V_h^0$ . Let us especially choose  $\nu = \Phi_h$  and write

$$k_h^2 = \frac{\int_{\Omega} |\nabla \Phi_h|^2 \, d\Omega}{\int_{\Omega} \Phi_h^2 \, d\Omega} = \frac{|\Phi_h|_{H^1}^2}{\|\Phi_h\|_{L_2}^2}. \quad (11)$$

Taking square roots of each side of (11) expresses  $k_h$  in terms of  $H^1$  seminorm and  $L_2$  norm of the corresponding eigenfunction. Similar derivation can be done for the exact eigenvalue

$$k^2 = \frac{\int_{\Omega} |\nabla \Phi|^2 \, d\Omega}{\int_{\Omega} \Phi^2 \, d\Omega} = \frac{|\Phi|_{H^1}^2}{\|\Phi\|_{L_2}^2}. \quad (12)$$

For the relative error in  $k_h$ , we get

$$\frac{|k_h - k|}{|k|} = \frac{\left| \frac{|\Phi_h|_{H^1}}{\|\Phi_h\|_{L_2}} - \frac{|\Phi|_{H^1}}{\|\Phi\|_{L_2}} \right|}{\frac{|\Phi|_{H^1}}{\|\Phi\|_{L_2}}}. \quad (13)$$

Write  $\|\Phi_h\|_{L_2} = (1 + \varepsilon_1)\|\Phi\|_{L_2}$  and  $|\Phi_h|_{H^1} = (1 + \varepsilon_2)|\Phi|_{H^1}$ . The numbers  $\varepsilon_1$  and  $\varepsilon_2$  are very small, typically less than  $10^{-4}$  and  $10^{-2}$ , respectively. Thus,

$$\frac{1}{\|\Phi_h\|_{L_2}} = \frac{1}{\|\Phi\|_{L_2}} \frac{1}{1 + \varepsilon_1} \approx \frac{1}{\|\Phi\|_{L_2}} (1 - \varepsilon_1). \quad (14)$$

Inserting (14) into (13), we get to the first order in  $\varepsilon_1$

$$\frac{|k_h - k|}{|k|} = \frac{||\Phi_h|_{H^1} - |\Phi|_{H^1} - \varepsilon_1|\Phi_h|_{H^1}|}{|\Phi|_{H^1}}. \quad (15)$$

Using triangle inequality of real numbers and  $\mathbf{H}^1$  seminorm, we have

$$\begin{aligned} \frac{|k_h - k|}{|k|} &\leq \frac{|\Phi_h - \Phi|_{H^1}}{|\Phi|_{H^1}} + |\varepsilon_1| \frac{|\Phi_h|_{H^1}}{|\Phi|_{H^1}} \\ &= \frac{|\Phi_h - \Phi|_{H^1}}{|\Phi|_{H^1}} + |\varepsilon_1|(1 + \varepsilon_2). \end{aligned} \quad (16)$$

Dropping the term  $\varepsilon_1\varepsilon_2$  and applying the triangle inequality of  $\mathbf{L}_2$  norm in  $\varepsilon_1$ , we finally get

$$\frac{|k_h - k|}{|k|} \leq \frac{|\Phi_h - \Phi|_{H^1}}{|\Phi|_{H^1}} + \frac{||\Phi_h - \Phi||_{L_2}}{||\Phi||_{L_2}}. \quad (17)$$

In (17), the second term is the relative  $\mathbf{L}_2$  error of the approximating eigenfunction. For a singular problem, the  $\mathbf{L}_2$  error is much less than the error in  $\mathbf{H}^1$  seminorm (which is close to the error in full  $\mathbf{H}^1$  norm) (see Table I).

We conclude that for the approximation of the eigenvalue  $k$  in Helmholtz equation (6), we are mostly concerned in bounding the error of the modal solution in  $\mathbf{H}^1$  seminorm, or almost equivalently, in the  $\mathbf{H}^1$  norm.

Thus, for conducting wedge problems, Table I suggests that a polynomial basis may yield poor results for the eigenvalues due to poor approximation properties in the  $\mathbf{H}^1$  norm. Instead, the extended basis has much better approximation properties, especially in  $\mathbf{H}^1$ . These remarks depend on how dominating the wedges in the whole problem are. In a corrugated waveguide, for example, there are many wedges, and polynomials are expected to yield rather inaccurate results.

#### IV. NUMERICAL RESULTS

We test our new basis by solving cutoff frequencies ( $f_c$ ) and wavenumbers ( $K_c$ ) for five waveguide structures, which have been dealt with in the literature. The structures are as follows.

*Example I:* Fin line discussed in [33].

*Example II:* Rectangular vaned waveguide discussed in [34] and [19].

*Example III:* Single-ridged waveguide discussed in [34] and [18].

*Example IV:* Double-ridged waveguide discussed in [18] and several others

*Example V:* Quadruple-ridged waveguide discussed in [18] and several others.

In example I, the symmetry has been exploited, and one-quarter of the structure has been discretized by nine elements, as shown in Fig. 4. The problem contains one singularity of order  $\nu = 1/2$ . Table II presents these results.

Except for [33], the same geometrical mesh has been used for all results in Table II. The variable order meshes used are shown in Fig. 5. For "Ext-1, variable order," we chose  $p_{\max} = 6$  and for "Polynomial, variable order,"  $p_{\max} = 8$ . Note that the values from [33] have been corrected by a factor of  $2.9979/3$  because more accurate value for the speed of light should be used. Convergence to five digits is obtained in all Ext-1 cases, where the complete polynomial part is at least sixth order. Ext-1 appears

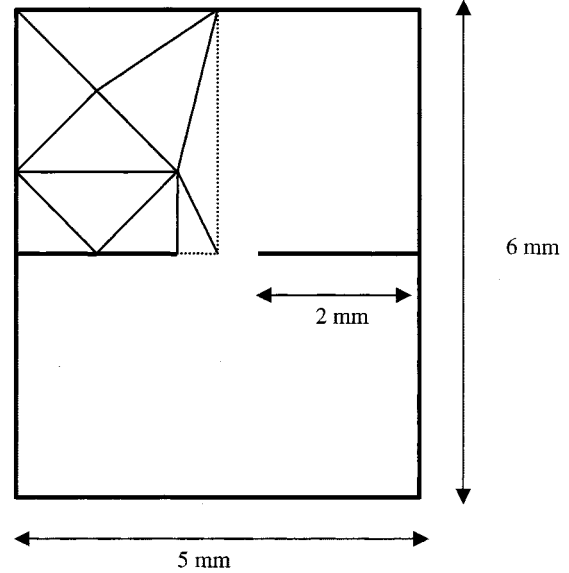


Fig. 4. Structure and mesh in example I.

TABLE II  
VALUES OF CUTOFF FREQUENCIES (IN GIGAHERTZ) FOR THE FIRST SINGULAR TM MODE AND TWO FIRST SINGULAR TE MODES IN EXAMPLE I (FIN LINE) [DEGREES OF FREEDOM (d.o.f.)]

|                            | d.o.f. | TM <sub>1</sub> | d.o.f. | TE <sub>1</sub> | d.o.f. | TE <sub>3</sub> |
|----------------------------|--------|-----------------|--------|-----------------|--------|-----------------|
| [33], FDTD                 | -      | 55.84           | -      | 15.92           | -      | 30.74           |
| Polynomial, $p=3$          | 36     | 56.427          | 48     | 16.338          | 45     | 30.900          |
| Ext-1, $p=3$               | 37     | 56.006          | 49     | 15.942          | 46     | 30.751          |
| Ext-12, $p=3$              | 38     | 56.004          | -      | -               | -      | -               |
| Ext-13, $p=3$              | 38     | 56.006          | 50     | 15.941          | 47     | 30.751          |
| Polynomial, $p=8$          | 276    | 55.911          | 308    | 15.984          | 300    | 30.764          |
| Ext-1, $p=8$               | 277    | 55.840          | 309    | 15.914          | 301    | 30.738          |
| Polynomial, variable order | 129    | 55.914          | 143    | 15.985          | 135    | 30.764          |
| Ext-1, variable order      | 89     | 55.842          | 103    | 15.914          | 97     | 30.738          |
| <b>Convergence</b>         |        | <b>55.840</b>   |        | <b>15.914</b>   |        | <b>30.738</b>   |

to be much more accurate than the polynomial basis alone. We observe also that maximal performance of both polynomial and extended bases can be exploited very efficiently using variable order meshes. Instead, introducing Ext-12 or Ext-13 bases almost does not make any difference to Ext-1. The same observation was made with all examples discussed below, thus, we leave Ext-12 and Ext-13 cases off the tables and suggest not using them.

In example II, one-half of the structure has been discretized by the six elements shown in Fig. 6. Again, there is one singularity of order  $\nu = 1/2$ . Table III presents the results. We obtained convergence to 2.0978 rad/cm while Gil *et al.* [19] reported a convergence value of 2.0981 rad/cm. Since the eigenvalue is approximated from above, we assume that our value is closer to the exact one. In any case, compared to [19],

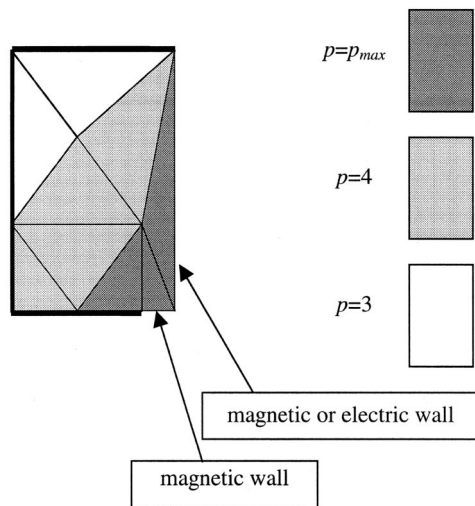


Fig. 5. Variable-order mesh in example I.

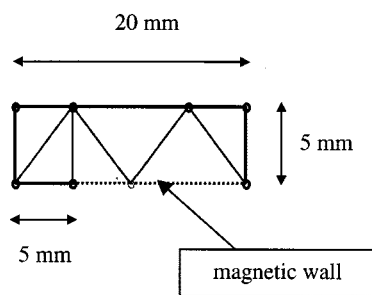


Fig. 6. Structure and mesh in example II.

TABLE III  
VALUES OF  $K_c$  (IN RADIAN PER CENTIMETERS) FOR THE FIRST SINGULAR TE MODE IN EXAMPLE II (VANED RECTANGULAR WAVEGUIDE) [DEGREES OF FREEDOM (d.o.f)]

|                                | d.o.f. | $K_c$         |
|--------------------------------|--------|---------------|
| Ext-1, $p_{max}=5$             | 48     | 2.0984        |
| Ext-1, $p_{max}=6$             | 67     | 2.0979        |
| Gil [19]                       | 70     | 2.0986        |
| Swaminathan [34]               | -      | 2.1156        |
| <b>Convergence (this work)</b> |        | <b>2.0978</b> |
| <b>Convergence (Gil [19])</b>  |        | <b>2.0981</b> |

with 70 degrees of freedom (d.o.f.), our result with 48 d.o.f. is slightly better, and with 67 d.o.f., is clearly better. Convergence to five digits is obtained in all Ext-1 cases, where the complete polynomial part is at least sixth order. The same convergence value was obtained using a uniform 32-element mesh and  $p = 8$  (1057 d.o.f.).

Example III has one plane of symmetry, and one-half of the structure is discretized by six elements (Fig. 7). Now there is one singularity of order  $\nu = 2/3$ . The results are given in Table IV. Similar comments are valid here than with example II. Using

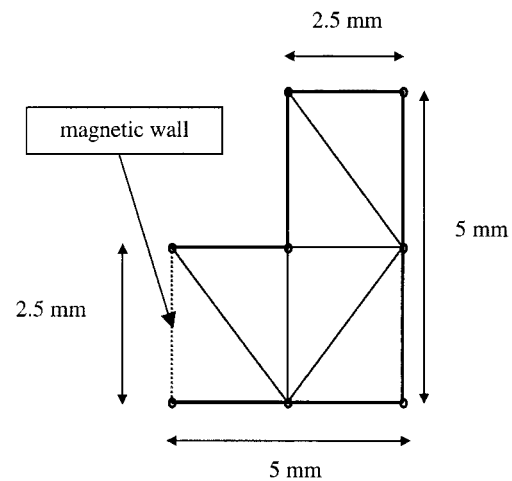


Fig. 7. Structure and mesh in example III.

TABLE IV  
VALUES OF  $K_c$  (IN RADIAN PER CENTIMETERS) FOR THE FIRST SINGULAR TE MODE IN EXAMPLE III (SINGLE RIDGE WAVEGUIDE) [DEGREES OF FREEDOM (d.o.f)]

|                                | d.o.f. | $K_c$         |
|--------------------------------|--------|---------------|
| Ext-1, $p_{max}=4$             | 47     | 2.2501        |
| Ext-1, $p_{max}=5$             | 60     | 2.2496        |
| Gil [19]                       | 58     | 2.2501        |
| Swaminathan [34]               | -      | 2.2496        |
| <b>Convergence (this work)</b> |        | <b>2.2495</b> |
| <b>Convergence (Gil [19])</b>  |        | <b>2.2497</b> |

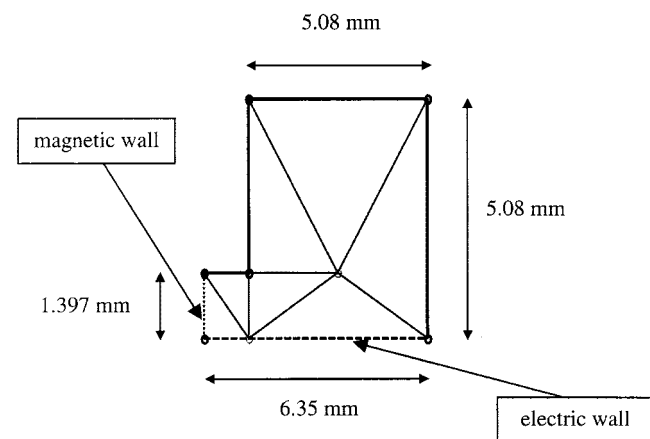


Fig. 8. Structure and mesh in example IV.

comparable amount of degrees of freedom than in [19], we obtain more accurate result (0.004% versus 0.03%). Convergence to five digits is obtained in all Ext-1 cases, where the complete polynomial part is at least fifth order.

Example IV has two planes of symmetry, and one-quarter of the structure is discretized by seven elements (Fig. 8). There is one singularity of order  $\nu = 2/3$ . The results are given in Table V. Our result with 40 d.o.f. is comparable to Gil's result

TABLE V  
VALUES OF  $K_c$  (IN RADIAN PER CENTIMETERS) FOR THE FIRST THREE TE  
MODES IN EXAMPLE IV (SYMMETRIC DOUBLE-RIDGED WAVEGUIDE)  
[DEGREES OF FREEDOM (d.o.f)]

|                    | d.o.f. | 1 <sup>st</sup> TE | 2 <sup>nd</sup> TE | 3 <sup>rd</sup> TE |
|--------------------|--------|--------------------|--------------------|--------------------|
| Ext-1, $p=3$       | 40     | 1.440              | 6.193              | 6.713              |
| Gil [18]           | 54     | 1.439              | 6.203              | 6.731              |
| Gil [18]           | 141    | 1.439              | 6.193              | 6.714              |
| <b>Convergence</b> |        | <b>1.438</b>       | <b>6.192</b>       | <b>6.711</b>       |

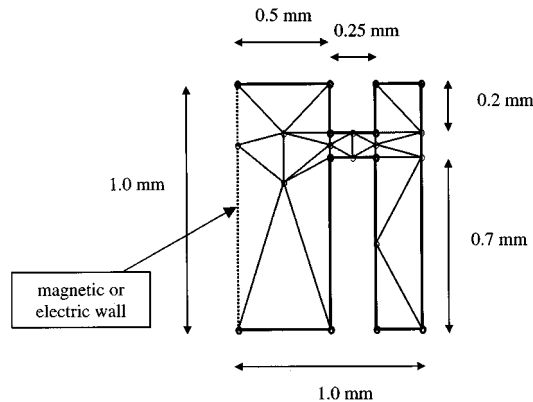


Fig. 9. Structure and mesh in example V.

TABLE VI  
VALUES OF  $K_c$  (IN RADIAN PER CENTIMETERS) FOR THE FIRST TWO TE  
MODES IN EXAMPLE V (SYMMETRIC QUADRUPLE-RIDGED WAVEGUIDE)  
[DEGREES OF FREEDOM (d.o.f)]

|                    | d.o.f. | 1 <sup>st</sup> TE | d.o.f. | 2 <sup>nd</sup> TE |
|--------------------|--------|--------------------|--------|--------------------|
| Ext-1, $p=3$       | 133    | 0.906              | 140    | 1.155              |
| Gil [18]           | 108    | 0.907              | 117    | 1.156              |
| <b>Convergence</b> |        | <b>0.904</b>       |        | <b>1.151</b>       |

with 141 d.o.f. Convergence to four digits is obtained in all Ext-1 cases, where the complete polynomial part is at least fifth order.

Finally, example V has one plane of symmetry, and one-half of the structure is discretized by 24 elements (Fig. 9). There are four singularities of order  $\nu = 2/3$ . The results are given in Table VI. Our result is comparable to Gil's result, ours being slightly more expensive. Convergence to four digits is obtained in all Ext-1 cases, where the complete polynomial part is at least fifth order. The reason for the relative expense of our result is that, in the algorithm, the supports of the extension functions must not overlap and, therefore, the elements close to the singular corners are necessarily small in this geometry. With high-order basis, the intention is to use large elements, but if the geometry requires "too" small elements, some efficiency of the high-order basis is lost.

## V. CONCLUSION

In this paper, an extension to a polynomial finite-element basis is proposed to better manage wedge singularities. An error estimate for the eigenvalues in the Helmholtz equation is given. It is shown that the error in  $k$  is essentially bounded by the  $H^1$  error of the numerical modal solution. Several numerical examples validate that the extended basis yields superior performance over polynomial basis, and compares well with the other recent extension techniques. Varying the order of the elements over the mesh yields an additional significant improvement. Loosely speaking, close to the singular tips, resolution of the field needs higher order polynomials, while far from the tips, the field is smooth and low-order polynomials suffice.

## ACKNOWLEDGMENT

The author acknowledges the Aristotle University of Thessaloniki, Thessaloniki, Greece, where most of this work was conducted.

## REFERENCES

- [1] D. M. Pozar, *Microwave Engineering*. Reading, MA: Addison-Wesley, 1990.
- [2] I. J. Bahl, *Microstrip Antennas*. Norwood, MA: Artech House, 1980.
- [3] J. Meixner, "The behavior of electromagnetic fields at edges," *IEEE Trans. Antennas Propagat.*, vol. AP-20, pp. 442–446, July 1972.
- [4] J. Van Bladel, "Field singularities at metal-dielectric wedges," *IEEE Trans. Antennas Propagat.*, vol. AP-33, pp. 450–455, Apr. 1985.
- [5] J. B. Andersen, "Field behavior near a dielectric wedge," *IEEE Trans. Antennas Propagat.*, vol. AP-26, pp. 598–602, July 1978.
- [6] W. E. Boyse and K. D. Paulsen, "Accurate solutions of Maxwell's equations around PEC corners and highly curved surfaces using nodal finite elements," *IEEE Trans. Antennas Propagat.*, vol. 45, pp. 1758–1767, Dec. 1997.
- [7] W. E. Boyse and A. A. Seidl, "A hybrid finite element method for 3-D scattering using nodal and edge elements," *IEEE Trans. Antennas Propagat.*, vol. 42, pp. 1436–1442, Oct. 1994.
- [8] K. B. Whiting, "A treatment for boundary singularities in finite difference solutions of Laplace's equation," *IEEE Trans. Microwave Theory Tech.*, vol. MTT-16, pp. 889–891, 1968.
- [9] D. B. Ingham, P. J. Heggs, and M. Manzoor, "Boundary integral equation analysis of transmission-line singularities," *IEEE Trans. Microwave Theory Tech.*, vol. MTT-29, pp. 1240–1243, Nov. 1981.
- [10] V. Postoyalko, "Green's function treatment of edge singularities in the quasi-TEM analysis of microstrip," *IEEE Trans. Microwave Theory Tech.*, vol. MTT-34, pp. 1092–1095, Nov. 1986.
- [11] Q. Xu, K. J. Webb, and R. Mittra, "Study of modal solution procedures for microstrip step discontinuities," *IEEE Trans. Microwave Theory Tech.*, vol. 37, pp. 381–387, Feb. 1989.
- [12] Z. Pantic and R. Mittra, "Quasi-TEM analysis of microwave transmission lines by the finite-element method," *IEEE Trans. Microwave Theory Tech.*, vol. MTT-34, pp. 1096–1103, Nov. 1986.
- [13] P. Tracey and T. Cook, "Analysis of power type singularities using finite elements," *Int. J. Numer. Methods Eng.*, vol. 11, pp. 1225–1233, 1977.
- [14] J. E. Akin, *Application and Implementation of Finite Element Methods*. New York: Academic, 1982.
- [15] P. P. Silvester and R. L. Ferrari, *Finite Elements for Electrical Engineers*. Cambridge, U.K.: Cambridge Univ. Press, 1996.
- [16] J. P. Webb, "Finite element analysis of dispersion in waveguides with sharp metal edges," *IEEE Trans. Microwave Theory Tech.*, vol. 36, pp. 1819–1824, Dec. 1988.
- [17] B. A. Szabó and I. Babuška, *Finite Element Analysis*. New York: Wiley, 1991.
- [18] J. M. Gil and J. Zapata, "Efficient singular element for finite element analysis of quasi-TEM transmission lines and waveguides with sharp metal edges," *IEEE Trans. Microwave Theory Tech.*, vol. 42, pp. 92–98, Jan. 1994.
- [19] —, "A new scalar transition finite element for accurate analysis of waveguides with field singularities," *IEEE Trans. Microwave Theory Tech.*, vol. 43, pp. 1978–1982, Aug. 1995.

- [20] R. De Smedt and J. Van Bladel, "Field singularities at the tip of a metallic cone of arbitrary cross section," *IEEE Trans. Antennas Propagat.*, vol. AP-34, pp. 865–870, July 1986.
- [21] E. Vafiadis and J. N. Sahalos, "Fields at the tip of an elliptic cone," *Proc. IEEE*, vol. 72, pp. 1089–1091, Aug. 1984.
- [22] D. R. Lynch and K. D. Paulsen, "Origin of vector parasites in numerical Maxwell solutions," *IEEE Trans. Microwave Theory Tech.*, vol. 39, pp. 383–394, Mar. 1991.
- [23] J. F. Lee, D. K. Sun, and Z. J. Cendes, "Full-wave analysis of dielectric waveguides using tangential vector finite elements," *IEEE Trans. Microwave Theory Tech.*, vol. 39, pp. 1262–1271, Aug. 1991.
- [24] —, "Tangential vector finite elements for electromagnetic field computation," *IEEE Trans. Magn.*, vol. 27, pp. 4032–4035, Sept. 1991.
- [25] Z. J. Cendes, "Vector finite elements for electromagnetic field computation," *IEEE Trans. Magn.*, vol. 27, pp. 3958–3966, Sept. 1991.
- [26] A. Chatterjee, J. M. Jin, and J. L. Volakis, "Computation of cavity resonances using edge-based finite elements," *IEEE Trans. Microwave Theory Tech.*, vol. 40, pp. 2106–2108, Nov. 1992.
- [27] I. Bardi, O. Biro, K. Preis, G. Vrisk, and K. R. Richter, "Nodal and edge element analysis of inhomogeneously loaded waveguides," *IEEE Trans. Magn.*, vol. 29, pp. 1466–1469, Mar. 1993.
- [28] G. Mur, "The finite-element modeling of three-dimensional electromagnetic fields using edge and nodal elements," *IEEE Trans. Antennas Propagat.*, vol. 41, pp. 948–953, July 1993.
- [29] A. F. Peterson, "Vector finite element formulation for scattering from two-dimensional heterogeneous bodies," *IEEE Trans. Antennas Propagat.*, vol. 43, pp. 357–365, Mar. 1994.
- [30] J. M. Gil and J. P. Webb, "A new edge element for the modeling of field singularities in transmission lines and waveguides," *IEEE Trans. Microwave Theory Tech.*, vol. 45, pp. 2125–2130, Dec. 1997.
- [31] Z. Pantic-Tanner, J. S. Savage, D. R. Tanner, and A. F. Peterson, "Two-dimensional singular vector elements for finite-element analysis," *IEEE Trans. Microwave Theory Tech.*, vol. 46, pp. 178–184, Feb. 1998.
- [32] G. Mur, "The modeling of singularities in the finite-difference approximation of the time-domain electromagnetic-field equations," *IEEE Trans. Microwave Theory Tech.*, vol. MTT-29, pp. 1073–1077, Oct. 1981.
- [33] P. Przybyszewski and M. Mrozowski, "A conductive wedge in Yee's mesh," *IEEE Microwave Guided Wave Lett.*, vol. 8, pp. 66–68, Feb. 1998.
- [34] M. Swaminathan, E. Arvas, T. K. Sarkar, and A. R. Djordjević, "Computation of cutoff wavenumbers of TE and TM modes in waveguides of arbitrary cross sections using a surface integral formulation," *IEEE Trans. Microwave Theory Tech.*, vol. 38, pp. 154–159, Feb. 1990.



**Jaakko S. Juntunen** was born in Tornio, Finland, in 1971. He received the Master of Science degree (with distinction) in technical mathematics and the Licentiate of Technology degree from the Helsinki University of Technology (HUT), Espoo, Finland, in 1995 and 1998, respectively, and is currently working towards the Dr.Sci. degree at HUT.

He is currently a Research Engineer in the Radio Laboratory, HUT. His current research interests are numerical dispersion and perfectly matched layers in FDTD method, the high-order FEM applied to electromagnetic problems and the method of moments (MoM).

Mr. Juntunen was awarded a position in the national graduate school GETA for 1996–2000. For the academic year 1998–1999 he was granted a European Union's Marie Curie Fellowship to work at the Aristotle University of Thessaloniki.

**Theodoros D. Tsiboukis** (S'79–M'81) was born in Larissa, Greece, on February 25, 1948. He received the Diploma degree in electrical and mechanical engineering from the National Technical University of Athens, Athens, Greece, in 1971, and the Dr. Eng. degree from the Aristotle University of Thessaloniki, Thessaloniki, Greece, in 1981.

During the 1981–1982 academic year, he was a Visiting Research Fellow in the Electrical Engineering Department, University of Southampton, U.K. Since 1982, he has been with the Department of Electrical and Computer Engineering, Aristotle University of Thessaloniki, where he is currently a Professor. From 1993 to 1997, he was the Director of the Division of Telecommunications, Department of Electrical and Computer Engineering, Aristotle University of Thessaloniki, and in 1997, was elected the Chairman of this Department from 1997 to 1999. He has authored six books, and has authored or co-authored over 60 refereed journal articles and over 50 conference papers. His research interests include electromagnetic-field analysis by energy methods, computational electromagnetics [FEM, boundary-element method (BEM), vector finite elements, MoM, FDTD, and absorbing boundary conditions (ABC's)], and adaptive meshing in FEM analysis. He was the guest editor of a special issue of the *International Journal of Theoretical Electrotechniques* (1996) and the chairman of the local organizing committee of the 8th International Symposium on Theoretical Electrical Engineering (1995). He is a member of various societies, associations, chambers, and institutions. He has also organized and chaired conference sessions.

Dr. Tsiboukis has been awarded a number of distinctions.